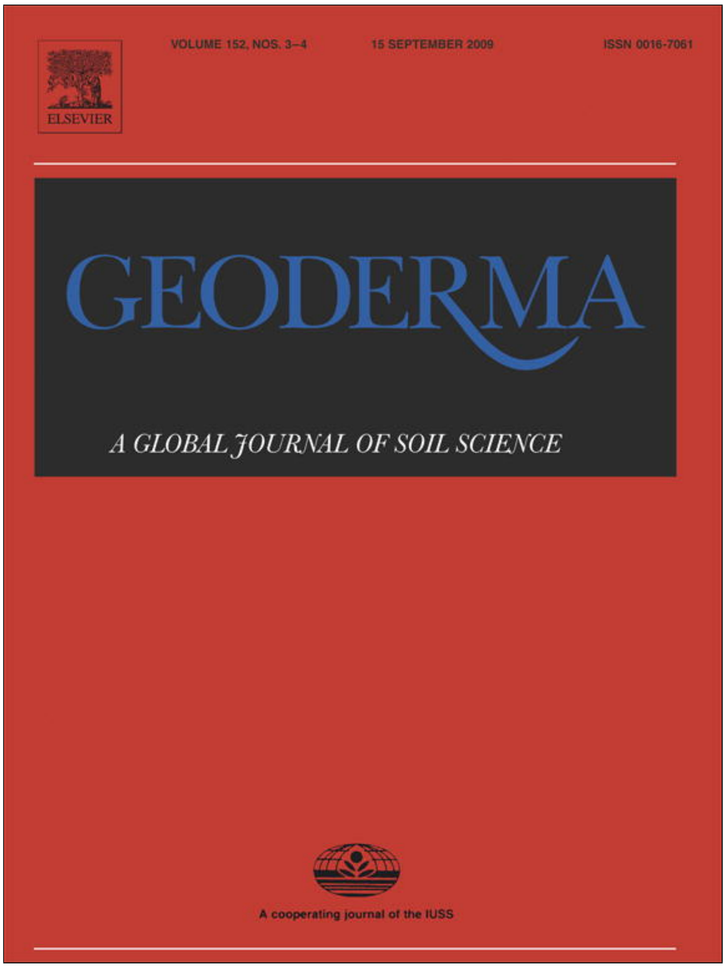
VOLUME 152, NOS. 3–4
15 SEPTEMBER 2009
ISSN 0016-7061
ELSEVIER
GEODERMA
A GLOBAL JOURNAL OF SOIL SCIENCE
A cooperating journal of the IUSS

Geoderma 152 (2009) 338–349

Contents lists available at ScienceDirect

Geoderma

journal homepage: www.elsevier.com/locate/geoderma

# Estimation of soil hydraulic properties using proximal spectral reflectance in visible, near-infrared, and shortwave-infrared (VIS–NIR–SWIR) region

Priyabrata Santra [a], Rabi Narayan Sahoo [b], Bhabani Sankar Das [a,*], Ravindra Nath Samal [c], Ajit Kumar Pattanaik [c], Vinod Kumar Gupta [b]

[a] *Agricultural and Food Engineering Department, Indian Institute of Technology, Kharagpur, West Bengal, 721302, India*
[b] *Division of Agricultural Physics, Indian Agricultural Research Institute, New Delhi, 110012, India*
[c] *Chilika Development Authority, C-11, BJB Nagar, Bhubaneswar, Orissa, 751014, India*

ARTICLE INFO

*Article history:*
Received 22 May 2008
Received in revised form 29 April 2009
Accepted 1 July 2009
Available online 24 July 2009

*Keywords:*
Pedotransfer functions
Spectrotransfer functions
Water retention parameters
Saturated hydraulic conductivity
Proximal spectral reflectance
VIS–NIR–SWIR

ABSTRACT

Characterization of soil hydraulic properties is an important step for assessing soil water regime in agricultural fields. Because direct measurement of soil hydraulic properties at multiple locations is costly and time-consuming, pedotransfer functions (PTF) are conveniently used to estimate these properties from easily measurable basic soil properties. Over the last two decades, several studies have demonstrated that basic soil properties of surface soils may be rapidly estimated by measuring soil spectral reflectance. In this study, we evaluated a PTF approach to use proximal spectral reflectance over the visible, near-infrared, and shortwave-infrared (VIS–NIR–SWIR) region (350–2500 nm) as predictor variable in place of basic soil properties. To develop these transfer functions, spectral reflectance of air-dried and sieved soil samples was measured using a handheld spectroradiometer equipped with a contact probe. Transfer functions in the form of multiple linear regression relationships between soil hydraulic properties and different attributes of measured spectral reflectance were developed. These new transfer functions are called spectrotransfer functions (STF). Both the parametric PTFs and STFs for the parameters of van Genuchten water retention model ($\alpha$ and $n$) and point PTF for saturated hydraulic conductivity ($K_s$) were evaluated using the root-mean-squared error (*RMSE*). Results show that STFs have the similar accuracy as PTFs for estimating hydraulic properties. Specifically, STFs developed with the absorption features of proximal spectral reflectance performed better than the PTFs for estimating $\alpha$. Among three hydraulic parameters for which the STFs were developed, van Genuchten parameter $n$ is well predicted with comparatively lower values of *RMSE*. Thus, this study shows that proximal spectral reflectance of soil may be used for rapid estimation of soil hydraulic properties in a large area with accuracy comparable to PTFs. A rigorous testing in different geographical regions is warranted to establish the utility of STFs as a method for estimating soil hydraulic properties.



## 1. Introduction

Water retention characteristics (relationship between volumetric water content, $\theta$ and matric potential head, $h$) and saturated hydraulic conductivity ($K_s$) are two soil hydraulic parameters required for assessing water regime in saturated and unsaturated soils. These two properties also serve as critical inputs for detailed hydrological models that are used for making water resource planning at various scales. Both these soil properties are spatially and temporally variable (Hills et al., 1992) and depend on a specific measurement method (Lee et al., 1985; Paige and Hillel, 1993). Estimation of hydraulic properties at multiple locations even within an agricultural field is time-consuming and costly (Romano and Palladino, 2002). Over the last few decades, the pedotransfer function (PTF) approach has been advocated as an alternative method for estimating soil hydraulic properties (Bouma, 1989; Rawls et al., 1991; Schaap et al., 1998; Wösten et al., 2001; McBratney et al., 2002; Pachepsky et al., 2006).

Typically, PTFs are expressed in terms of linear (Rawls et al., 1982; Vereecken et al., 1989; Tomasella and Hodnett, 1998) or non-linear (Scheinost et al., 1997; Wösten et al., 1999; Hodnett and Tomasella, 2002) regression equations using basic soil properties as predictor variables (Rawls et al., 1982; Vereecken et al., 1989; Tomasella and Hodnett, 1998; Wösten et al., 1999; Schaap et al., 2001). Recently, topographic features (Pachepsky et al., 2001; Romano and Palladino, 2002) and vegetation indices (Sharma et al., 2006) have also been considered as predictor variables in PTFs. Similarly, advanced modeling techniques such as artificial neural network (ANN) (Schaap et al., 1998; Tamari and Wösten, 1999; Schaap et al., 2001; Minasny and McBratney, 2002; Minasny et al., 2004; Jana et al., 2008) or k-nearest neighborhood (Nemes et al., 2006) approaches have been proposed.

* Corresponding author. Tel.: +91 3222 283162; fax: +91 3222 282244.
*E-mail address:* bsdas@iitkgp.ac.in (B.S. Das).

0016-7061/$ – see front matter 
doi:10.1016/j.geoderma.2009.07.001

The performance of several PTFs has also been compared with available measurement methods. For example, Šimunek et al. (1998) compared the hydraulic properties measured with the tension infiltrometer with those obtained from class PTFs (Carsel and Parrish, 1988) and ANN-based predictions (Schaap et al., 1998) and observed that the ANN-based approach may be used as an alternative to direct measurement of soil hydraulic properties. Similarly, Cornelis et al. (2001) showed that the PTFs developed by Vereecken et al. (1989) are better than nine different PTFs published in the literature. More recently, Jana et al. (2007) coupled the Bayesian ANN with a non-linear bias correction approach to predict soil hydraulic properties across multiple spatial scales. Despite these developments, large sets of input data are still needed to develop reliable PTFs. In addition, the PTFs also needed to be locally developed (Hodnett and Tomasella, 2002; Li et al., 2007). Creation of large soil database for region-specific PTF development is time-consuming and costly.

Over the last two decades, proximal spectral reflectance in the visible, near-infrared, and shortwave-infrared (VIS–NIR–SWIR) region (350–2500 nm) has been successfully used for accurate and rapid estimation of soil properties such as particle size distributions, organic matter contents, electrical conductivity, etc. (Henderson et al., 1989; Ben-Dor and Banin, 1995; Ben-Dor et al., 1997; Ben-Dor et al., 1999; Chang et al., 2001; Dunn et al., 2002; McCarty et al., 2002; Reeves et al., 2002; Shepherd and Walsh, 2002; Islam et al., 2003; Stevens et al., 2006; Viscara Rosel et al., 2006; Brown et al., 2006; Nanni and Demattê, 2006; Lagacherie et al., 2008). Estimation of soil properties via proximal spectral reflectance is a convenient and rapid field-scale measurement approach although it is applicable only to surface soil characterization (Ben-Dor et al., 1999). Recently, Ben Dor et al. (2008) reported the use of frequency domain electromagnetic radiation (FDEM) and ground penetrating radar (GPR) in addition to the VIS–NIR–SWIR spectral data for assessing soil salinity of subsurface soil. Inasmuch as basic soil properties may be estimated from proximal spectral reflectance, it is hypothesized that soil hydraulic properties may be related to spectral reflectance. Thus, similar to PTFs, spectro-transfer functions (STFs) may be developed to estimate hydraulic properties from spectral reflectance. However, STFs are also required to be locally developed and should be based on large training datasets on soil hydraulic properties and spectral reflectance data.

Only two studies indicate that hydraulic properties may be related to proximal spectral reflectance (Thine et al., 2004; Janik et al., 2007). Both of these studies do not explicitly provide STFs. Thine et al. (2004) characterized soil degradation using relationships between soil hydraulic properties and spectral reflectance over the VNIR region through the partial least square regression (PLSR) technique. Recently, Janik et al. (2007) have calibrated reflectance spectra in mid-infrared (MIR) region to estimate soil water content at various matric pressure heads using the PLSR technique. They also did not include the parametric approach for estimating soil water retention behaviour. Thus, the objective of the present study was to develop STFs for soil hydraulic properties from the proximal spectral reflectance data over the VIS–NIR–SWIR region and test their performance with PTFs.

## 2. Materials and methods

### 2.1. Study area and soil sampling

The experimental data used in this study were collected from the 'Dengei Pahad micro-watershed' (DPMW) (~42 km$^2$), which is a part of the western catchment of Chilika Lake system in Orissa, India (Santra, 2009). The DPMW lies between 19°49′48″–19°52′8.4″ N and 85°13′55.2″–85°14′34.8″ E. with elevations ranging from 27 to more than 85 m above mean sea level. The land-use classes of the watershed show 42% agricultural land, 22% forested area with evergreen and deciduous trees, and 36% wetlands with natural shrubs. Soil series level data for the study area (NBSS&LUP, 2005) at a scale of 1:250,000 show five dominant soil series with the Nuagarh series occupying about 62% area of the watershed. Soils of this watershed are classified as Typic Haplustalfs. Surface (0–10 cm depth) soil samples were collected from the DPMW in five sampling campaigns. Out of a total of 100 soil samples collected, 23 samples were collected on a 200 m × 600 m grid during the first sampling campaign and the rest of the samples were collected on a 1–2 km × 1–2 km grid. Soils at this site are generally sandy at high elevation areas and heavy clays at low-lying depression area. Agricultural land is confined to the lower reach of the watershed. Hill tops within the watershed are covered with sparse to dense vegetation.

During each sampling, undisturbed soil cores (5 cm internal diameter and 6 cm long) and approximately 500 g of loose soil from top 10 cm layer were collected from each grid point. Soils were air-dried, ground and shifted through a 2 mm sieve and stored for chemical, physical, and spectral analysis. Processed soils were analyzed to determine particle density ($\rho_p$), bulk density ($\rho_b$), organic carbon contents (OC) and particle size distribution using pycnometer method (Flint and Flint, 2002), core method (Blake and Hartge, 1986), the chromic acid digestion method (Walkley and Black, 1934), and the international pipette method (Gee and Bauder, 1986), respectively. Soil pH and electrical conductivity (EC) were measured in 1:2.5 soil: water slurry. Saturated hydraulic conductivity ($K_s$) was determined using a constant head permeameter (Eijelkamp Agrisearch Equipment, Netherlands) (Klute and Dirksen, 1986). Measurements were taken both in 'constant head' and 'falling head' modes depending on soil texture. For heavy clay soils, only the falling head method was adopted. For each soil sample, $K_s$ measurements were repeated three times.

Water retention behaviour of each soil sample was determined using a tempecell setup connected to a pressure plate manifold. Water contents were measured in soil cores (5 cm in diameter, 6 cm long) at successive equilibrium pressures of 10, 20, 30, 40, 50, 60, 70 and 80 kPa. Pressure head-water content ($h-\theta$) data for different soil samples were fitted to the van Genuchten water retention model (Van Genuchten, 1980):

$$S_e = \left(\frac{\theta-\theta_r}{\theta_s-\theta_r}\right) = \left[\frac{1}{1+(\alpha|h|)^n}\right]^{1-\frac{1}{n}} \tag{1}$$

where $S_e$ is the relative saturation, $\theta_r$ is the residual soil water content (cm$^3$ cm$^{-3}$), $\theta_s$ is the saturated soil water content (cm$^3$ cm$^{-3}$), $h$ is the matric potential head (cm) and $\alpha$ (cm$^{-1}$) and $n$ are shape parameters of the water retention curve. Eq. (1) was used to estimate the van Genuchten retention model parameters $\theta_r$, $\alpha$ and $n$ for each soil sample using the SOLVER function of the EXCEL spreadsheet Program. Parameter $\theta_s$ was equated to soil porosity and was used as a constant in Eq. (1).

### 2.2. Spectral reflectance of soil in VIS–NIR–SWIR region

Proximal spectral reflectance of processed soil samples (air-dried and ground soil samples sifted through 2 mm sieve) were recorded in the VIS–NIR–SWIR region (350–2500 nm) in the laboratory using a portable spectroradiometer (Model: Field spec®3 FR, Analytical Spectral Devices Inc., USA). All spectral measurements were recorded using a contact probe having 10 mm spot size and its own light source with a 1500 h halogen bulb. The use of contact probe minimizes errors associated with stray light during measurements under solar illumination. Proximal spectral reflectance of each soil sample was recorded with respect to a 5″ × 5″ white reference (spectralon) panel (Labsphere, North Sutton, USA). Spectral reflectance data for each soil sample was generated by arithmetic averaging of 60 replicated measurements for that sample. The reference panel reflectance was measured before each sample measurement. Three main features of the proximal spectral reflectance spectra were used for analysis: a) individual proximal spectral reflectance values [$R(\lambda)$] for each wavelength, b) integrated proximal spectral reflectance values (hereinafter, referred to as band reflectance) for a selected wave bands, and c) continuum removal (*CR*) factor around absorption bands. The band reflectance values were estimated by integrating $R(\lambda)$ values over the bandwidths used in the Enhanced Thematic Mapper Plus (ETM+) sensor onboard Landsat-7 satellite. The ETM+ sensors collect data over six VIS–NIR–SWIR regions and one thermal region. The spectral bands corresponding to ETM+ bands used in this study are: 450–520 nm (ETM+1), 520–600 nm (ETM+2), 630–690 nm (ETM+3), 760–900 nm (ETM+4), 1550–1750 nm (ETM+5), and 2080–2350 nm (ETM+7). Hereinafter, these six bands are referred to as band-1 to band-6, respectively. The spectroradiometer-measured $R(\lambda)$ values were integrated over these six bands using the following relationship:

$$R_i = \frac{\sum_{\lambda u_i}^{\lambda l_i} R(\lambda)\phi_i(\lambda)}{\sum_{\lambda u_i}^{\lambda l_i} \phi_i(\lambda)} \tag{2}$$

where $R_i$ is the calculated *i*th band reflectance, $\lambda u_i$ is the upper boundary of band *i*, $\lambda l_i$ is the lower boundary of band *i*, $R(\lambda)$ is the reflectance for wavelength *i*, $\phi(\lambda)$ is the spectral response function of band *i*.

The raw soil spectra followed the same basic shape as described by other researchers (Ben-Dor et al., 1999; Shepherd and Walsh, 2002) with prominent absorption features around 1400, 1900, and 2200 nm (Chang et al., 2001; Shepherd and Walsh, 2002; Lagacherie et al., 2008). Significant variation in these three absorption features among soil samples was also observed. The absorption features around 1400 and 1900 nm are associated with OH functional group of free water (Shepherd and Walsh, 2002) and the absorption around 2200 nm is associated with OH functional group of clay lattice (Chabrillat et al., 2002; Lagacherie et al., 2008). As these three absorption features are strongly related with either free water or lattice water, therefore, these may not suitably be used in remotely sensed data where atmospheric water vapour may weaken the signal/noise ratio or in field condition where soil water content is highly variable. However, these absorption features for a grounded and air-dried soil may be characteristic of specific soil type and, hence, may be linked with the typical water retention behaviour of a soil. Therefore, we have selected these three absorption features to be included as predictor variables for estimation of soil hydraulic properties. The *CR* factors are a unique way to characterize these absorption features (Lagacherie et al., 2008). Before calculating the CR factors, $\lambda_{peak}$, $\lambda_{min}$, and $\lambda_{max}$ of each absorption feature and corresponding reflectance [$R(\lambda_{peak})$, $R(\lambda_{min})$ and $R(\lambda_{max})$] were identified. The first derivative of spectral reflectance around absorption features of each soil sample showed spikes and low with $dR/d\lambda \approx 0$ for a particular wavelength, which is considered as peak wavelength ($\lambda_{peak}$). The mean of $\lambda_{peak}$ for all soil samples showed the absorption peaks at 1414 nm, 1913 nm, and 2207 nm wavelengths with standard deviation of ±2 nm. For each absorption feature, two local maxima ($\lambda_{min}$ and $\lambda_{max}$) on both sides of $\lambda_{peak}$ were identified using the inflection point of the reflectance spectra ($d^2R/d\lambda^2$). The mean local maxima corresponding to each absorption feature were observed to be 1329 and 1615 nm, 1860 and 2125 nm, and 2125 and 2257 nm, respectively. After identification of $\lambda_{peak}$, $\lambda_{min}$, and $\lambda_{max}$, corresponding reflectance values were extracted from spectral data of each soil sample. The position of $\lambda_{peak}$, $\lambda_{min}$, and $\lambda_{max}$ for each absorption feature in few selected reflectance spectra is shown in Fig. 1. The *CR* factor was calculated from $R(\lambda_{peak})$, $R(\lambda_{min})$ and $R(\lambda_{max})$ of each absorption band using the following relationship:

$$CR_\lambda = \min\left[1, \frac{R\left(\lambda_{peak}\right)}{R(\lambda_{max}) + \frac{\lambda_{min}-\lambda_{peak}}{\lambda_{min}-\lambda_{max}}\left[R(\lambda_{min}) - R(\lambda_{max})\right]}\right] \tag{3}$$

where, $R(\lambda_{peak})$ is the reflectance at $\lambda_{peak}$, $R(\lambda_{min})$ is the reflectance at $\lambda_{min}$, and $R(\lambda_{max})$ is the reflectance at $\lambda_{max}$. The calculated *CR* factors for three absorption peaks at 1414 nm, 1913 nm, and 2207 nm are referred to as $CR_{1414}$, $CR_{1913}$, and $CR_{2207}$.

### 2.3. Development of PTF

Before proceeding to PTF development, descriptive statistics of the measured soil properties, band reflectance, and *CR* factors were calculated. Each variable was checked for normality at 5% level of significance using the Kolmogorov–Smirnov (K–S) test statistics. Necessary transformations were made for the variable, which did not follow normal distribution. Basic soil properties, proximal spectral reflectance, integrated band reflectance, and *CR* factors were correlated with soil hydraulic properties using Spearman correlation statistics. Basic soil properties, proximal spectral reflectance, integrated band reflectance, and *CR* factors were used as separate set of predictor variables for PTF/STF development. Besides these four sets, integrated band reflectance and *CR* factors were taken together in a separate set. Therefore, a total of five sets of predictor variables were formulated for PTF/STF development.

To reduce the heterodasticity in the dataset, stepwise regression analysis and principal component analysis (PCA) were done. In stepwise regression analysis, important predictor variables were identified at 5% level of significance. Principal component analysis is generally applicable for data with high dimension and large interdependency between data dimensions. Therefore, application of PCA with proximal spectral reflectance and integrated band reflectance spectra is more meaningful. But to maintain similarity in the analysis, PCA was applied to each set of predictor variables. Principal components, which describe about 95% of the total variation in data, were considered in final reduced data. The Eigen value of each principal component indicates the amount of variation in the dataset explained by that particular principal component. To establish the physical significance of the principal components, relationship between original variables and Eigenvectors, commonly referred to as factor loadings, were checked (Hair et al., 1995). The original variables with large absolute value of factor loadings for a given principal component determine its physical significance. As a result of the stepwise regression and PCA analysis, each set of predictor variables was divided into three subsets. The first subset consists of all predictor variables of main set. The second subset consists of important predictor variables in stepwise analysis. The third subset consists of major principal components obtained after PCA of all predictor variables in the main set. With full reflectance spectra, only the set of major principal components obtained through PCA were used as predictor variables. Therefore, a total of thirteen subsets of predictor variables (three subsets from each of the first, second, third and fourth set and one from the fifth set) were formulated for PTF development.

The total dataset ($N=100$) was randomly divided into development dataset and validation dataset at a ratio of 3:1. The development dataset was used for developing the PTFs whereas the validation dataset was used for testing the performance of the PTFs. A point PTF for $\ln(K_s)$ and parametric PTFs for the van Genuchten parameters, $\alpha$ and $n$, were developed through multiple linear regression equation of the form,

$$Y = a_0 + \sum_{k=1}^{k} a_k X_k \tag{4}$$

where *Y* is the dependent variable, $X_k$ is the *k*th independent variable (input), $a_0$, $a_1$, $a_2$, …, $a_k$ are regression coefficients and *k* is the number of independent variable in regression equation. The basic soil properties and spectral information were taken as independent variable and the hydraulic properties [$\ln(K_s)$, $\ln(\alpha)$, and $n$] were taken as dependent variables in the Eq. (4) for developing PTFs/STFs. The multiple linear regression equations were developed using the *regress* function of MATLAB software.

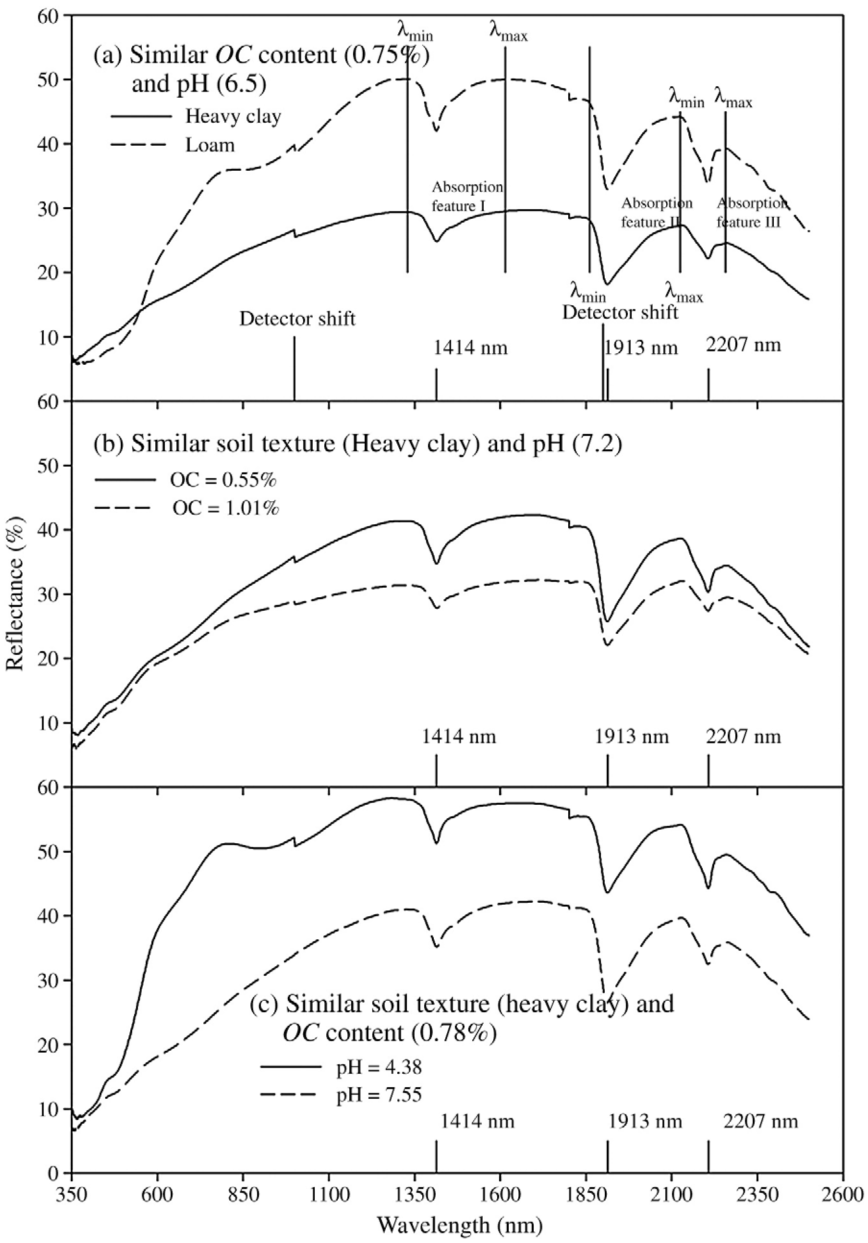


**Fig. 1.** Reflectance spectra of soil samples (a) for two soil textural classes with similar OC content and pH and (b) for different organic carbon content with similar soil texture and pH, and (c) for different pH with similar soil texture and OC content.

To reduce the uncertainty of the predicted hydraulic parameters, PTFs were developed from 500 realizations of the development dataset through boot-strapping (Efron and Tibshirani, 1993). In this procedure, random subsets of the original development database of the same size are created through sampling with replacement. Each sample has a chance of $1-[(N-1)/N]^N$ to be selected once or multiple times for a particular subset resulting in subsets that contain about 63% unique cases from the original data. Thus, each boot-strapped database may be viewed as a subset of the original development database containing 47 unique samples and 28 repeated samples from the original database. Multiple linear regression equations were developed for each replica database. Thus, for a given hydraulic parameter we obtained 500 regression equations:

$$Y_j = a_{0j} + \sum_{k=1}^{k} a_{kj} X_k \quad (5)$$

where $j$ ranged from 1 to 500. The coefficients $a_0$ and $a_\mathrm{k}$ were obtained from arithmetic average of 500 coefficients:

$$a_0 = \frac{1}{500}\sum_{j=1}^{500} a_{0j} \quad \text{and} \quad a_k = \frac{1}{500}\sum_{j=1}^{500} a_{kj}. \quad (6)$$

Following the multiple linear regression approach with boot-strapping as stated above, PTFs were developed with thirteen subsets of predictor variables that were initially formulated.

Performance of PTFs was evaluated in validation dataset. Root-mean-squared error (*RMSE*) was used as the evaluation index:

$$RMSE = \sqrt{\frac{1}{N-p}\sum_{i=1}^{N}\left(Y_i - \hat{Y}_i\right)^2} \quad (7)$$

where, $p$ is the number of independent variables used in the PTF model. To test the efficacy of VIS–NIR–SWIR reflectance spectra as predictor for estimating hydraulic properties, performance of reflectance spectra-based PTFs were compared with basic soil property-based PTFs. Hereinafter, the reflectance spectra-based PTFs are referred to as spectrotransfer functions (STF) for soil hydraulic properties as suggested by Lagacherie et al. (2008).

## 3. Results and discussion

### 3.1. Soil properties and spectral information

Different physical, chemical, and spectral properties of soils collected from the DPMW watershed are summarized in Table 1. Soils at this site had wide variation in physical and chemical properties as is expected in a hillslope catena. For example, soil $\rho_p$ ranged from 2.40 to 3.00 g cm$^{-3}$ with the mean $\rho_p$ (2.55 g cm$^{-3}$) less than the particle density (2.65 g cm$^{-3}$) generally assumed for mineral soils. Similarly, the mean $\rho_b$ was 1.51 g cm$^{-3}$ while $\rho_b$ ranged from 1.80 to 2.00 g cm$^{-3}$ for the red colored soils of high elevation areas and pastures. Very loose soils of sandy clay loam texture with $\rho_b$ as low as 1.00–1.20 g cm$^{-3}$ were also observed for few cultivated areas. Mean OC content of the soil samples was high (>0.75%) as per the rating for Indian soils (ICAR, 2006). Sand and clay contents also varied widely within the watershed. Sand contents were observed to increase with elevation and the reverse was true for clay contents. Particle density showed the same trend with elevation possibly because of a strong correlation between $\rho_p$ and sand content. A total of seven different textural classes were observed in this watershed although the majority of soil samples had either light clay texture having clay content >25% ($N=36$) or heavy clay texture having clay content >45% ($N=25$) indicating the presence of fine textured soils in the study area. Soils were generally acidic with pH values being as low as 3.44 because of the presence of Fe- and Al-oxides. Saturated hydraulic conductivity also showed wide variation ($K_s>1000$ cm day$^{-1}$ for coarse textured soils and $K_s<0.1$ cm day$^{-1}$ for heavily textured soils). The van Genuchten parameter, $\alpha$ was log-normally distributed with a mean value of $-2.26$. The mean value for the other van Genuchten parameter, $n$ was 1.22. Kolmogorov–Smirnov test revealed that except for EC, $K_s$, and $\alpha$, all other soil properties were normally distributed at 5% level of significance.

Proximal spectral reflectance for each soil sample generally increases in the visible range and plateaus to a maximum value between 1500 and 1700 nm before it again decreases in the SWIR range. Each spectrum also shows characteristic reduction in spectral reflectance around 1414, 1913, and 2207 nm wavelength. Fig. 1 shows the specific change in these characteristics as influenced by texture (Fig. 1a), OC content (Fig. 1b), and pH (Fig. 1c). These figures show that the overall brightness decreases with the increase in fineness in soil texture (Fig. 1a) and pH (Fig. 1c). The increase in brightness with increase in fineness of particles was also reported by previous researchers (Ben-Dor et al., 2003; Goldshleger et al., 2004). Greater brightness of the reflection spectra for acidic soils may be due to the red coloration imparted by chromophores like Fe- and Al-oxides (Leone and Sommer, 2000). Fig. 1b shows that soil OC content influences the reflection spectra primarily in the 1000–1900 nm because of absorption of shortwave infrared (SWIR) radiation by OC content.

Both band reflectance and *CR* factors obtained from proximal spectral reflectance data were normally distributed as observed from results of Kolmogorv–Smirnov test. Wide variation in each of six band reflectance and three *CR* factor was observed. Lower value of *CR* factor was observed for $CR_{1913}$ compared to $CR_{1414}$ and $CR_{2207}$. Variation of $CR_{1913}$ among soil samples is also highest among three *CR* factors. This indicates that $CR_{1913}$ is the most prominent absorption feature in the reflectance spectra.

### 3.2. Correlation among reflectance spectra, basic soil properties, and hydraulic properties

The effects of different soil properties on the proximal spectral reflectance are further explored using correlation analysis. Fig. 2 shows that soil $\rho_p$ shows maximum correlation ($r=-0.49$) with the spectral reflectance at 415 nm (Fig. 2a). Beyond 600 nm, $\rho_p$ does not show any correlation with the exception in absorption bands. Similarly, OC contents show maximum correlation ($r=0.18$) with the spectral reflectance at 1829 nm. The amount of coarse (sand) and fine (silt and clay) soil particles present in a soil shows good correlation with spectral reflectance (Fig. 2b); the correlation coefficients were positive for the coarse fraction and negative for the fine fractions. Fig. 2b shows that an increase in fineness of soil texture due to dominance of silt and clay particles in soil may decrease spectral reflectance. Similar trend may also be seen in Fig. 1a. Stronger correlation may also be observed between soil separates and the absorption bands (Fig. 2b). This result suggests that the proximal spectral reflectance may be used as a substitute variable for sand, silt, and clay content of soil. Similarly, Fig. 2c shows that both soil pH and EC are positively correlated with spectral reflectance at the blue region and negatively correlated for the rest of the spectrum. This figure also indicates that a decrease in pH and EC may increase spectral reflectance beyond 700 nm wavelength. The correlation of spectral reflectance with soil pH and EC also indicates the possible substitution of soil physiochemical properties with proximally measured spectral

**Table 1**
Descriptive statistics of soil properties and spectral information.

| Soil properties and spectral information | Minimum | Maximum | Mean | Standard deviation | Skewness | Kurtosis |
|---|---|---|---|---|---|---|
| Particle density (g cm$^{-3}$) | 2.30 | 3.03 | 2.55 | 0.14 | 1.08 | 4.66 |
| Bulk density (g cm$^{-3}$) | 1.11 | 2.00 | 1.51 | 0.18 | 0.09 | 2.81 |
| Organic carbon content (%) | 0.07 | 2.10 | 0.93 | 0.38 | 0.39 | 3.46 |
| Sand content (%) | 7.85 | 84.66 | 48.71 | 17.80 | −0.11 | 2.26 |
| Silt content (%) | 4.40 | 37.38 | 16.70 | 6.02 | 0.36 | 3.15 |
| Clay content (%) | 4.60 | 63.97 | 34.59 | 14.77 | 0.00 | 2.00 |
| pH (−) | 3.44 | 8.72 | 6.76 | 1.29 | −0.62 | 2.55 |
| ln(EC) (dS m$^{-1}$) | 0.002 | 1.31 | 0.14 | 1.13 | −1.11 | 6.53 |
| ln($K_s$) (cm day$^{-1}$) | −0.82 | 6.26 | 3.19 | 1.69 | −0.28 | 2.39 |
| ln($\alpha$) (cm$^{-1}$) | −5.81 | 1.51 | −2.26 | 1.44 | −0.04 | 2.82 |
| $n$ (−) | 1.03 | 1.54 | 1.22 | 0.09 | 1.00 | 4.42 |
| Band-1 (450–520 nm) | 5.11 | 21.55 | 13.25 | 3.71 | −0.05 | 2.68 |
| Band-2 (520–600 nm) | 8.73 | 32.34 | 19.02 | 5.01 | 0.36 | 3.09 |
| Band-3 (630–690 nm) | 11.83 | 42.59 | 24.61 | 6.21 | 0.62 | 3.38 |
| Band-4 (760–900 nm) | 16.96 | 50.85 | 32.04 | 7.29 | 0.35 | 2.77 |
| Band-5 (1550–1750 nm) | 19.63 | 60.40 | 43.07 | 8.83 | −0.14 | 2.38 |
| Band-6 (2080–2350 nm) | 16.47 | 54.27 | 37.50 | 8.35 | −0.20 | 2.48 |
| $CR_{1414}$ | 0.55 | 0.93 | 0.83 | 0.06 | −1.32 | 6.79 |
| $CR_{1913}$ | 0.46 | 0.87 | 0.70 | 0.07 | 0.13 | 3.64 |
| $CR_{2207}$ | 0.54 | 0.91 | 0.81 | 0.07 | −1.12 | 4.71 |

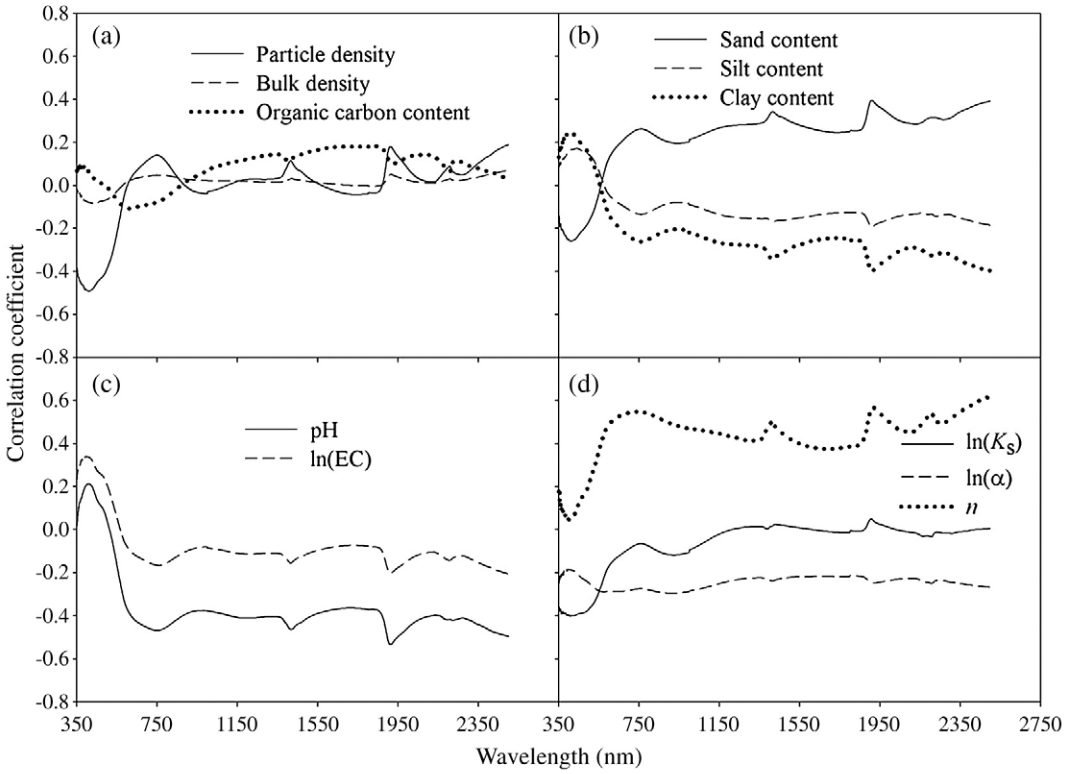


**Fig. 2.** Correlation coefficients between soil properties and proximal spectral reflectance at different wavelengths.

data. Similar observation was also pointed out earlier from Fig. 1c as an effect of soil pH on reflectance spectra. High correlation between basic soil properties and proximal spectral reflectance is also reported by several researchers (Leone and Sommer, 2000; McCarty et al., 2002; Odlare et al., 2005; Mouazen et al., 2007).

Because we intend to estimate soil hydraulic properties from proximal spectral reflectance data, correlation between spectral reflectance and soil hydraulic parameters was also explored. Among three soil hydraulic parameters, ln($K_s$) shows good correlation with spectral reflectance in the blue region whereas van Genuchten parameters (In (α) and $n$) show good correlation at 700–2500 nm wavelength (Fig. 2d). Another significant observation from correlation analysis (Fig. 2) is that both basic and soil hydraulic properties show large correlation coefficients (Table 2) with the proximal spectral reflectance values over a wide range (band) of wavelength suggesting the possibility of characterizing soil properties based on band reflectance in addition to reflectance at each wavelength values. Specifically, we observed high correlation of basic soil and hydraulic properties over blue, green, red, IR, SWIR, and 2000–2300 nm wavelength bands. The ETM+ sensor uses all these six bands (ETM + 1 to ETM + 5 and ETM + 7). Correlation coefficients listed in Table 2 suggest that the band reflectance in ETM + 1 and ETM + 2 bands are significantly correlated with ln($K_s$); band reflectance at all six bands were significantly correlated with van Genuchten parameters, ln(α) and $n$. Similarly, we also observed good correlation between soil hydraulic properties and absorption bands. Among $CR$ factors of three absorption bands, $CR_{1913}$ was significantly correlated with most soil properties ($r$>0.35); $CR_{1414}$ and $CR_{2207}$ were also correlated with $\rho_p$ ($r$ = 0.42 and 0.20, respectively) and clay content ($r$ = −0.36 and −0.19, respectively). Overall, correlation analysis suggests that spectral information is comparable to basic soil properties in terms of correlation with soil hydraulic properties.

**Table 2**
Correlation coefficient of basic soil properties, band reflectance, and continuum removal factors with soil hydraulic parameters.

| Soil properties and spectral information | ln($K_s$) | ln($a$) | $n$ |
|---|---|---|---|
| Particle density (g cm$^{-3}$) | 0.43** | 0.07 | 0.41** |
| Bulk density (g cm$^{-3}$) | −0.25* | −0.46** | 0.21* |
| Organic carbon content (%) | −0.05 | 0.00 | −0.16 |
| Sand content (%) | 0.50** | −0.03 | 0.56** |
| Silt content (%) | −0.21* | −0.03 | −0.35** |
| Clay content (%) | −0.51** | 0.05 | −0.54** |
| pH (−) | −0.14 | 0.19 | −0.46** |
| ln(EC) (dS m$^{-1}$) | −0.26* | −0.14 | −0.23* |
| Band-1 (450–520 nm) | −0.37** | −0.24** | 0.20 |
| Band-2 (520–600 nm) | −0.25* | −0.29** | 0.42** |
| Band-3 (630–690 nm) | −0.11 | −0.29** | 0.53** |
| Band-4 (760–900 nm) | −0.09 | −0.29** | 0.53** |
| Band-5 (1550–1750 nm) | 0.00 | −0.22* | 0.38** |
| Band-6 (2080–2350 nm) | −0.02 | −0.24* | 0.50** |
| $CR_{1414}$ | 0.06 | −0.12 | 0.46** |
| $CR_{1913}$ | 0.19 | −0.19 | 0.60** |
| $CR_{2207}$ | −0.07 | −0.13 | 0.36** |

*, and ** indicate correlation coefficients which are significant at 5%, and 1% level of significance respectively.

### 3.3. Stepwise regression and principal component analysis

Scatter plots and correlation analyses showed that several input variables are correlated among themselves which is generally termed as heterodasticity. Such heterodasticity in the data was eliminated through the stepwise regression analysis and PCA before PTF/STF development. Results of the stepwise regression analysis at 5% significance level showed that out of all the basic soil properties clay contents, $\rho_b$, and $\rho_p$ are the important predictor variables for ln($K_s$). Similarly, integrated band reflectance values corresponding to ETM + 1 and ETM + 7 bands (band-1 and band-6) were the important predictor variables for ln($K_s$) out of six band reflectance and band reflectance plus 3 $CR$ factors. It was also observed that none of the three $CR$ factors were significant predictor variables for ln($K_s$) at 5% significance level, but $CR_{1913}$ and $CR_{2207}$ were significant at 10% level of significance. The stepwise regression analysis for ln(α) showed that $\rho_b$, ln(EC), and pH are important predictor variables among basic soil properties; integrated band reflectance corresponding to ETM + 2 (band-2) was the only important predictor variable out of six band reflectance and their combination with the *CR* factors. In case of *CR* factors for $\ln(\alpha)$, none was selected at 5% level except $CR_{1913}$ was important at 10% level of significance. Similarly, sand content and pH were observed to be the important predictor variables for $n$ among the basic soil properties; band reflectance corresponding to ETM + 3 and ETM + 1 (band-3 and band-1) were important predictor variables among the six band reflectance values; and $CR_{1913}$ and integrated band reflectance for ETM + 4 (band-4) were the important predictor variables out of the combination of band reflectance and *CR* factors. In case of *CR* factors for $n$, $CR_{1913}$ was only selected at 5% level of significance.

Major principal components along with the associated factor loadings for each variable i.e. integrated band reflectance values, *CR* factors, band reflectance plus *CR* factors, and proximal spectral reflectance in VIS–NIR–SWIR region are presented in Fig. 3. The factor loadings of variables for each principal component indicate the importance of that variable to the said principal component. The PCA of eight basic soil properties showed six major principal components (data not shown in Fig. 3) suggesting that measured basic soil properties are almost orthogonal (linearly independent) to each other. In contrast, six band reflectance values were reduced to two major principal components explaining 94.7% variation of the dataset as indicated by the associated Eigenvalues. The first principal component of band reflectance values had positive and similar loading for each band. Therefore, the reflectance for each wavelength contributes equally to the first major principal component and hence may be considered as representation of the height of reflectance spectra or the overall spectral brightness. Similarly, the second principal component represents the slope of reflectance spectra by showing maximum value corresponding to band-1 and band-5. Previous investigations also reported that the first two major principal components of spectral reflectance describe the overall brightness and slope of the reflectance spectra (Leone and Sommer, 2000). The PCA with three *CR* factors resulted in two principal components explaining 99.4% variation of dataset. The first principal component of three *CR* factors represents $CR_{1913}$ and $CR_{2207}$ factors, whereas the second principal component represents all the three factors. Combination of band reflectance and *CR* factors were reduced to three principal components explaining 96.7% variation of data. The first principal component was equally contributed by six band reflectance and three *CR* factors as shown by equal amount of factor loadings in Fig. 3c. The proximal spectral reflectance data of 2150 dimensions were reduced to three major principal components explaining 98.5% variation of the dataset. Similar to the principal components of integrated band reflectance, the first and second principal components of proximal spectral reflectance indicate the overall brightness and slope of reflectance spectra, respectively. The third principal component captures

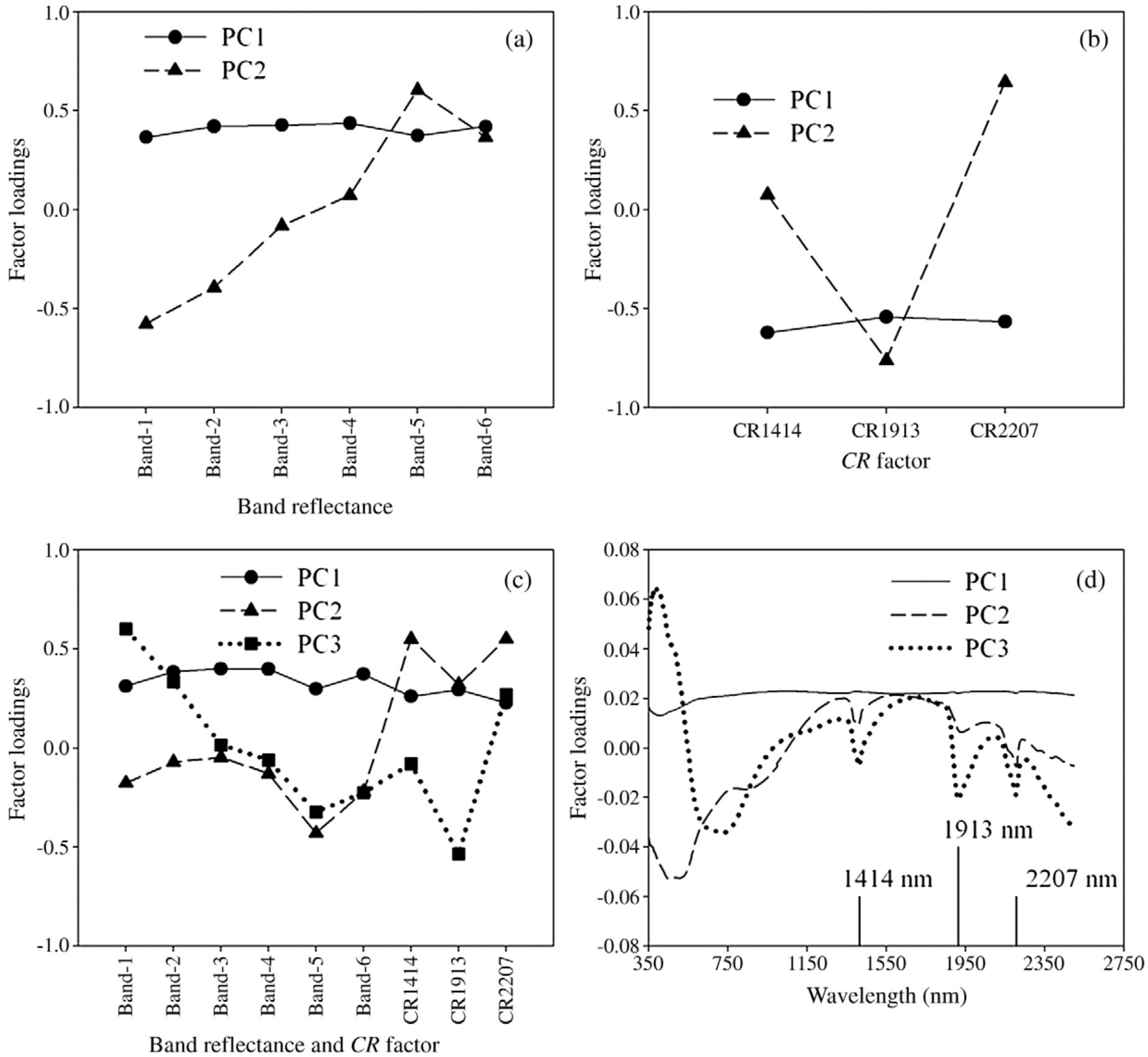


**Fig. 3.** Factor loadings of (a) band reflectance, (b) *CR* factors, (c) band reflectance plus CR factors, and (d) spectral reflectance at each wavelength for major principal components obtained after principal component analysis.

absorption features of reflectance spectra as shown by comparatively higher loadings corresponding to absorption peak. Thus, the major principal components of proximal spectral data and the derived spectral indices represent the characteristic features of the reflectance spectra i.e. overall brightness of the spectral reflectance curve, slope of the spectral reflectance curve, and absorption features of the spectral reflectance curve. Similar type of relationship between principal components and the characteristics features of spectral reflectance curve were reported by Leone and Sommer (2000).

### 3.4. Transfer functions and their performance

The stepwise regression analysis and PCA allowed us to develop PTFs and STFs using three critical subsets (without stepwise regression and PCA, with stepwise regression, and with PCA) of five main sets of input variables i.e. basic soil properties, band reflectance, *CR* actors, band reflectance plus *CR* factors, and spectral reflectance. Performance of PTFs/STFs were evaluated using the validation dataset ($N = 25$) in terms of *RMSE*. Results are summarized in Fig. 4. The first

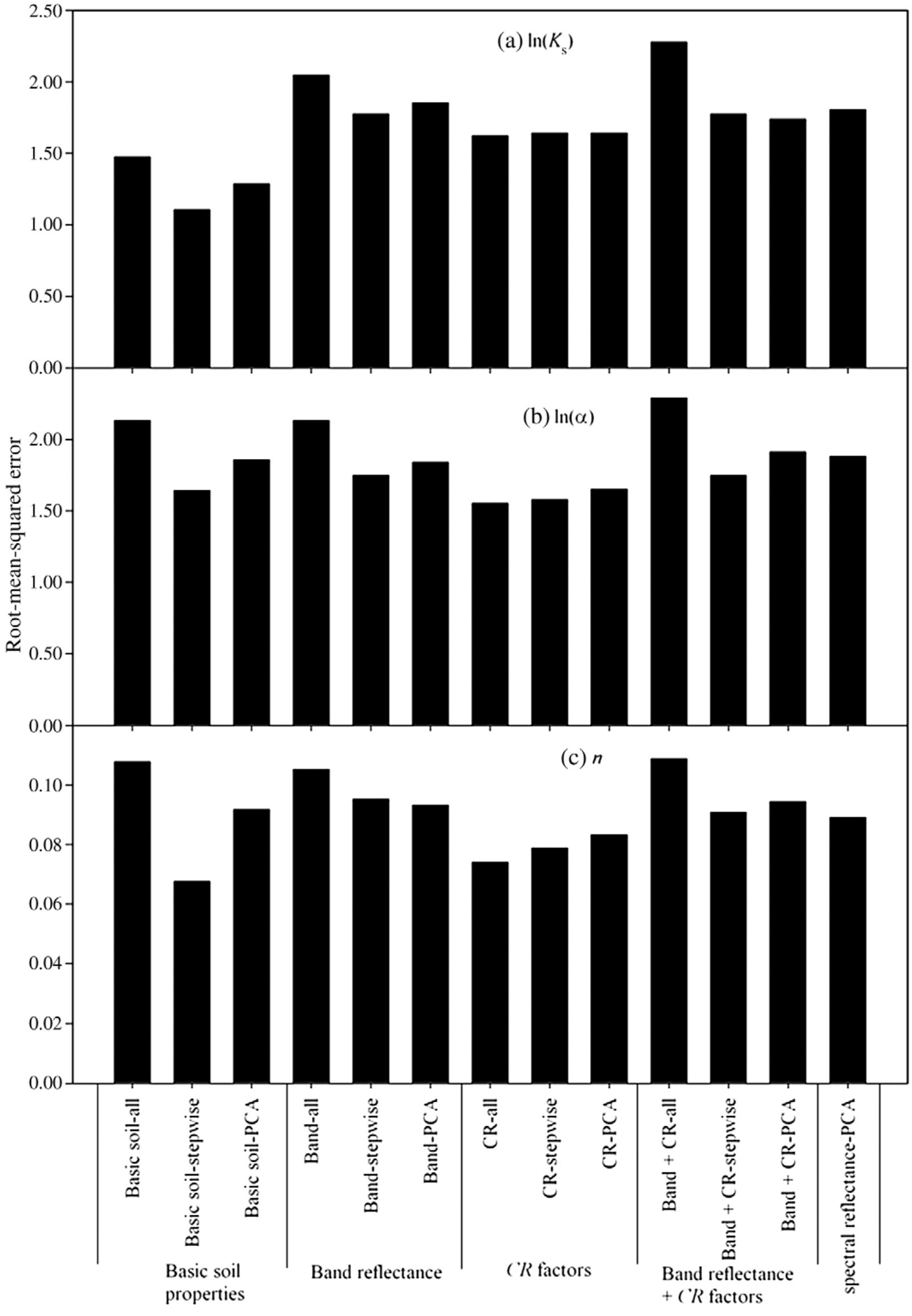


**Fig. 4.** Root-mean-squared error (*RMSE*) for pedotransfer functions and spectrotransfer functions for (a) saturated hydraulic conductivity [$\ln(K_s)$], (b) van Genuchten parameter [$\ln(\alpha)$], and (c) van Genuchten parameter ($n$), developed with different combination of predictor variables from basic soil properties, band reflectance, *CR* factors, band reflectance plus *CR* factors, and spectral reflectance. The suffixes “all”, “stepwise” and “PCA” of the *X*-axis labels indicate the PTFs/STFs developed with all predictor variables, after stepwise regression analysis, and after principal component analysis.

group (placed between two vertical line below *X*-axis) in the left side of Fig. 4 shows the performances of the PTFs, whereas remaining four groups show the performances of STFs. For estimating ln($K_s$), PTFs perform better than STFs. This was expected because $K_s$ is largely dependent on $\rho_b$ and spectral information was poorly correlated with $\rho_b$ in our study (Fig. 2). The PTFs developed with basic soil properties obtained through the stepwise regression analysis perform best among all PTFs/STFs. The STFs developed with *CR* factors perform next to PTFs in estimating ln($K_s$). For estimating ln($\alpha$), the STFs developed with *CR* factors performed better than other PTFs/STFs. The best performance in estimating ln($\alpha$) was observed when all three *CR* factors were used for the development of STF. The PTF developed with basic soil properties obtained through the stepwise regression analysis performed next to STFs developed with *CR* factors. For estimating *n*, the PTF developed with basic soil properties obtained through the stepwise regression performed best. The STFs developed with *CR* factors performed next to the best PTF in estimating *n*. Overall, the performances of STFs developed with *CR* factors performed better than other PTFs/STFs. In general, the best performance was achieved when all three *CR* factors were considered for PTF development. The PTFs/STFs developed with the set of predictor variables consisting of both band reflectance and *CR* factors performed worst because of over-fitting of redundant data.

Comparative study on performance of PTFs/STFs developed with reduced number of predictor variables through the stepwise regression analysis and PCA revealed that the stepwise regression yielded better result than PCA in most cases. Better performance of PTFs/STFs developed with predictor variables obtained in the stepwise regression may be due to removal of predictor variables which are not significantly correlated with hydraulic properties and, therefore, eliminating the insignificant variables in the dataset. Although, there is a possibility of removing theoretically highly correlated variables in stepwise analysis, it is preferred for dataset with low dimension. Whenever data dimension is very large, PCA or partial least square regression may be preferred (e.g., in cases of full reflectance spectra).

In this study, PTFs/STFs were developed with five different sets of predictor variables keeping in mind their availability from different sources for future applications. The PTFs may be used where dataset on specific soil properties are available. For developing countries where soil database is scarce, STFs may be used by utilizing the band reflectance data collected by the remote sensing satellites. But such application may be restricted in arid or semi-arid regions or for region where large portions of land kept under ploughing condition for certain period of time (Leone and Sommer, 2000). Specifically, the STFs based on the *CR* factors obtained from proximally measured spectral reflectance curve may not be translated with remote sensing data on spectral because two *CR* factors ($CR_{1414nm}$ and $CR_{1913nm}$) considered in this study correspond to water absorption bands and will be affected by the presence of water vapour in atmosphere. Therefore, *CR* factors or full reflection spectra may be used as predictor variables when reflectance spectra are available from the handheld or in some cases, from air-borne sensors. In case of application of STFs involving principal components as predictor variables, it may be calculated first by calculating matrix of standard normal variate of original variables followed by multiplying it with corresponding factor loadings matrix. With this anticipation, we have listed, the best PTF/STF from each five set of predictor variables in Table 3.

The prediction of hydraulic properties through PTFs/STFs may sometimes be insensitive to predictor variables even with lower value of *RMSE* in an independent dataset. Therefore, visual inspection of 1:1 plot of observed and predicted values of hydraulic properties is important to test the performance of PTFs. In our study, we have shown scatter plots of observed and predicted values with two extreme cases in performances for each hydraulic property (Fig. 5). The PTFs/STFs with best and worst performances were selected based on *RMSE* of each hydraulic property in validation dataset. From Fig. 5, it is found that scatter points of observed and predicted values of hydraulic properties are close to 1:1 line for cases with the best performances of PTFs/STFs and reasonable spread around 1:1 line even for cases with worst performances of PTFs/STFs. Among three hydraulic parameters, ln($\alpha$) was not estimated well by either PTF or STF even with the best cases. The developed PTFs from the same soil database in a previous study also showed poor performance of ln($\alpha$) in comparison to In($K_s$), and *n* (Santra and Das, 2008). The performance of the best PTFs/STFs developed in this study was also compared with reported established PTFs and was found better in each case.

## 4. Summary and conclusions

This study was carried out to develop transfer functions for soil hydraulic properties using spectral reflectance data collected over visible, near-infrared, and shortwave-infrared region of electromagnetic spectrum. One hundred surface soil samples collected from a micro-watershed near Chilika Lake were used for this study. Because these soils were collected from a hillslope, there was wide variation in soil properties. For example, soils contained seven dominant textural classes, had organic carbon contents ranging from 0.07 to 2.10%, pH ranging from 3.44 to 8.72 among others. Similarly, saturated hydraulic

**Table 3**
Pedotransfer and spectrotransfer functions for estimating saturated hydraulic conductivity and van Genuchten parameters from basic soil properties, and spectral reflectance of soil in visible and near-infrared region.

| Hydraulic parameter | Predictor variables in PTF/STF | Pedotransfer and spectrotransfer functions |
|---|---|---|
| ln($K_s$) | Basic soil properties | $1.5988-0.0408\times\text{Clay}-3.171\times\rho_b-3.0153\times\rho_p$ |
| | Band reflectance + *CR* | $3.041-0.1549\times\text{PC1}+0.117\times\text{PC2}-0.8867\times\text{PC3}$ |
| | Band reflectance | $4.7038-0.3397\times\text{Band-1}+0.0754\times\text{Band-6}$ |
| | *CR* factors | $3.925+10.7504\times CR_{1414}+3.3991\times CR_{1913}-15.0937\times CR_{2207}$ |
| | ASD full spectrum | $3.0416-0.006\times\text{PC1}+0.0673\times\text{PC2}-0.0453\times\text{PC3}$ |
| ln($\alpha$) | Basic soil properties | $3.9112-3.8758\times\rho_b+4.3657\times\ln(\text{EC})+0.4012\times\text{pH}$ |
| | Band reflectance + *CR* | $0.4533-0.1439\times\text{Band-2}$ |
| | Band reflectance | $0.4533-0.1439\times\text{Band-2}$ |
| | *CR* factors | $-0.0969+35.5831\times CR_{1414}-20.2724\times CR_{1913}-22.0356\times CR_{2207}$ |
| | ASD full spectrum | $-2.2427-0.0158\times\text{PC1}+0.0238\times\text{PC2}+0.004\times\text{PC3}$ |
| *n* | Basic soil properties | $1.298+0.0022\times\text{Sand}-0.0265\times\text{pH}$ |
| | Band reflectance + *CR* | $0.6623+0.5928\times CR_{1913}+0.0047\times\text{Band-4}$ |
| | Band reflectance | $1.2238+0.0232\times\text{PC1}+0.0166\times\text{PC2}$ |
| | *CR* factors | $0.614+0.8818\times CR_{1913}$ |
| | ASD full spectrum | $1.225+0.0013\times\text{PC1}-0.0002\times\text{PC2}-0.0041\times\text{PC3}$ |

Sand = sand content (%); Clay = clay content (%); $\rho_b$ = bulk density (g cm$^{-3}$); $\rho_p$ = particle density (g cm$^{-3}$); EC = electrical conductivity of soil (dS m$^{-1}$); pH = soil reaction in 1:2.5 soil solution; Band-1, Band-2, Band-4, and Band-6 are the band reflectance in 450–520 nm, 520–600 nm, 760–900 nm, and 2080–2350 nm, respectively; PC1, PC2, and PC3 are first, second, and third principal components respectively obtained after principal component analysis of respective high dimensional predictor variables; $CR_{1414nm}$, $CR_{1913}$, and $CR_{2207}$ are continuum removal factors at 1414 nm, 1913 nm, and 2207 nm respectively.

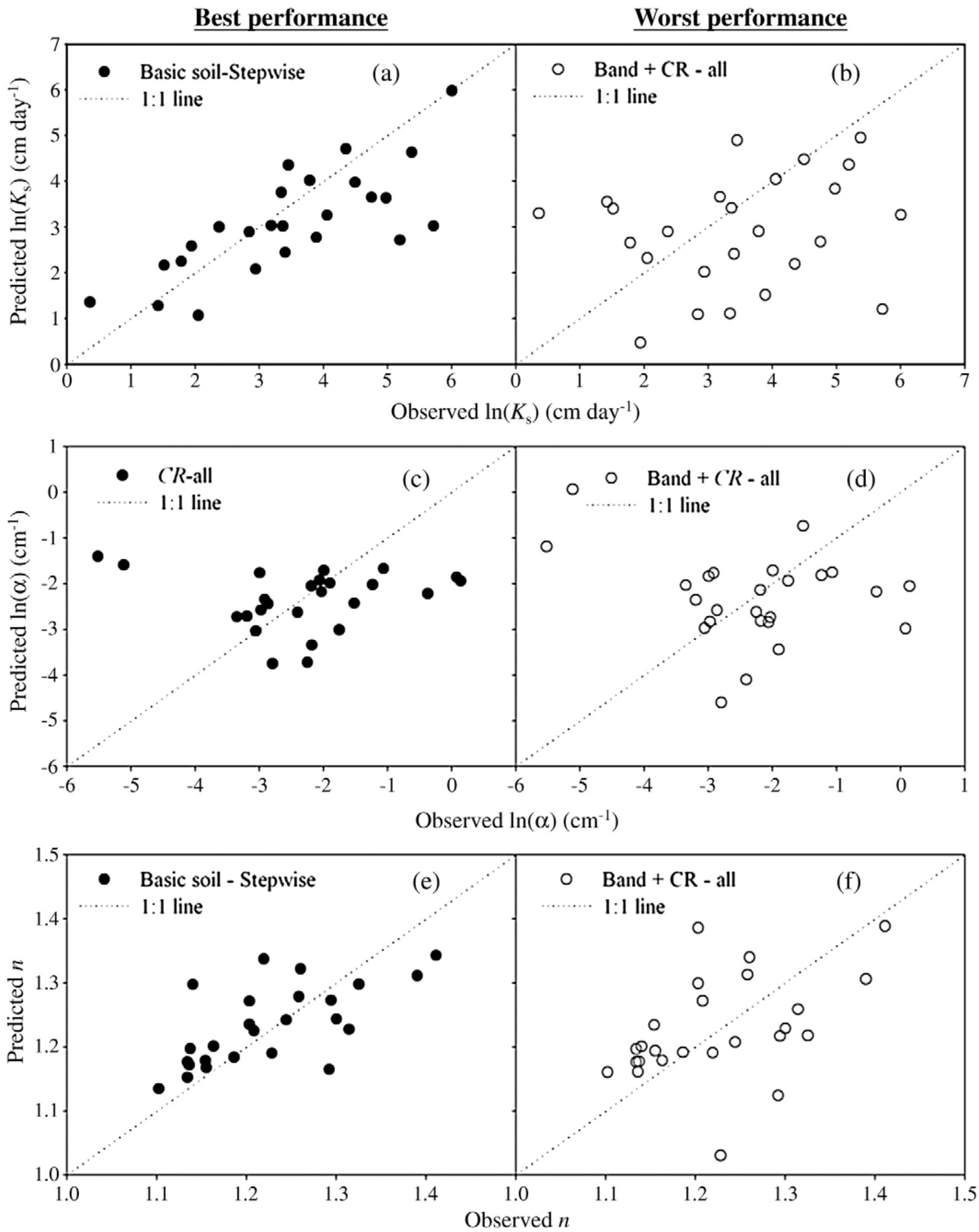


**Fig. 5.** Observed and predicted values of saturated hydraulic conductivity [ln($K_s$)] (a and b), and van Genuchten parameters, ln($\alpha$) (c and d), and van Genuchten parameter, $n$ (e and f) with the best performances (left side) and worst performances (right side) among pedotransfer functions and spectrotransfer functions developed with different combination of predictor variables for each hydraulic property.

conductivity of soils varied in four orders of magnitude. The van Genuchten parameter, $\alpha$ was log-normally distributed with a mean value of −2.26 with a coefficient of variation 63.72%. The mean value for the other van Genuchten parameter, $n$ was 1.22 with a coefficient of variation 7.11%. Such wide variation in basic and soil hydraulic properties are ideal for developing transfer functions for soil hydraulic properties (Santra and Das, 2008).

Proximal spectral reflectance of soils at VIS–NIR–SWIR region of the spectrum showed three characteristics features: overall brightness of the reflectance spectra, slope of the reflectance spectra from visible to near infrared, and three prominent absorption features at 1414 nm, 1913 nm, and 2207 nm. These features were well correlated to basic soil properties. For example, percent reflectance at the wavelength for most regions of reflectance spectra was significantly correlated ($|r|$ = 0.3 to 0.6) with particle size distribution, pH, EC, and van Genuchten parameters. Specifically, we observed high correlation of basic soil and hydraulic properties with spectral reflectance over blue, green, red, IR, SWIR, and 2000–2300 nm wavelength bands. Such correlation results allowed us to develop pedotransfer and spectrotransfer functions for soil hydraulic properties. Both point PTFs/STFs [for ln($K_s$)] and parametric PTFs/STFs [for van Genuchten parameter ln($\alpha$) and $n$] were developed by combining advanced statistical techniques such as stepwise multiple regression, boot-strapping, and principal component analyses. Developed PTFs/STFs were validated using a validation dataset. Results show that although the performance of STFs is not comparable with the PTFs for estimating hydraulic properties, but may be applied in case of unavailability of PTFs. In some cases, the STFs perform comparable to PTFs. Specifically, STFs developed with $CR_{1414}$, $CR_{1913}$, and $CR_{2207}$ performed similar to PTFs developed with basic soil properties; STF developed with $CR$ factors performed better than the PTFs for estimating $\alpha$. Among three hydraulic properties studied here, van Genuchten parameter $n$ is well predicted by STFs. With comparable performance of STFs with PTFs, STFs have the added advantage of being more easily developed because of the possibility of rapidly collecting spectral data compared to basic soil data. Moreover, spectral data may be collected over a large surface area and may be suitable for getting area-averages of hydraulic properties.

A specific limitation of this study is that the STFs were developed using air-dried and disturbed soil samples collected from top 10 cm soil surface. True structural attributes of soil are typically not fully retained in loose and disturbed soil samples. Thus, the STFs developed in this may be applicable only to surface soils. Future work is needed to examine if the STFs may be developed from undisturbed soil samples. Second, it may be possible that the transfer functions for soil hydraulic properties may be developed from the signatures of non-invasive methods such as FDEM and GPR sensors, which can measure soil properties in deeper soils (Ben Dor et al., 2008). Furthermore, the six wave bands selected for the analysis of the proximal reflectance data are the wave bands used in the ETM+ sensors onboard remote sensing satellites. This suggests that, if rigorously evaluated, the method outlined here may be suitable for large scale applications via direct measurements through remote sensing. Finally, a rigorous testing in different geographical regions is warranted to establish the utility of STFs as a method for estimating soil hydraulic properties.

## Acknowledgements

The senior author acknowledges the Indian Council of Agricultural Research, New Delhi for granting permission for study leave at IIT, Kharagpur.

## References

Ben-Dor, E., Banin, A., 1995. Near infrared analysis as a rapid method to simultaneously evaluate several soil properties. Soil Sci. Soc. Am. J. 59, 364–372.

Ben-Dor, E., Inbar, Y., Chen, Y., 1997. The reflectance spectra of organic matter in the visible near-infrared and short wave infrared region (400–2500 nm) during a controlled decomposition process. Remote Sens. Environ. 61, 1–15.

Ben-Dor, E., Irons, J., Epema, G., 1999. Soil spectroscopy, In: Rencz, A. (Ed.), Manual of Remote Sensing, 3rd edn. John Wiley and Sons, New York, pp. 111–188.

Ben-Dor, E., Gollshleger, N., Benyamini, Y., Agassi, M., Blumberg, D.G., 2003. The spectral reflectance properties of soil structural crusts in the 1.2- to 2.5-μm spectral region. Soil Sci. Soc. Am. J. 67, 289–299.

Ben Dor, E., Goldshleger, N., Eshel, M., Mirablis, V., Bason, U., 2008. Combined active and passive remote sensing methods for assessing soil salinity. In: Metternicht, G., Zinck, A. (Eds.), Remote Sensing of Soil Salinization: Impact on Land Management. CRC Press, USA, pp. 235–258.

Blake, G.R., Hartge, K.H., 1986. Bulk density. In: Klute, A. (Ed.), Methods of Soil Analysis, Part 1, Agronomy Monograph No. 9. ASA and SSSA, pp. 363–375. Madison, WI.

Bouma, J., 1989. Using soil survey data for quantitative land evaluation. Adv. Soil Sci. 9, 117–123.

Brown, D.J., Shepherd, K.D., Walsh, M.G., Dewayne Mays, M., Reinsch, T.G., 2006. Global soil characterization with VNIR diffuse reflectance spectroscopy. Geoderma 132, 273–290.

Carsel, R.F., Parrish, R.S., 1988. Developing joint probability distributions of soil water retention characteristics. Water Resour. Res. 24, 755–769.

Chabrillat, S., Goetz, A.F.H., Krosley, S., Olsen, H.W., 2002. Use of hyperspectral images in the identification and mapping of expansive clay soils and the role of spatial resolution. Remote Sens. Environ. 82, 431–445.

Chang, C., Laird, D.A., Mausbach, M.J., Hurburgh, C.R., 2001. Near-infrared reflectance spectroscopy — principal component regression analyses of soil properties. Soil Sci. Soc. Am. J. 65, 480–490.

Cornelis, W.M., Ronsyn, J., van Meirvenne, M., Hartmann, R., 2001. Evaluation of pedotransfer functions for predicting the soil moisture retention curve. Soil Sci. Soc. Am. J. 65, 638–648.

Dunn, B.W., Beecher, H.G., Batten, G.D., Ciavarella, S., 2002. The potential of near-infrared reflectance spectroscopy for soil analysis — a case study from the Riverine Plain of south-eastern Australia. Aust. J. Exp. Agric. 42 (5), 607–614.

Efron, B., Tibshirani, R.J., 1993. An introduction to the bootstrap. Monographs on Statistics and Applied Probability, vol. 57. Chapman and Hall, London, UK.

Flint, A.L., Flint, L.E., 2002. Particle density. In: Dane, J.H., Topp, G.C. (Eds.), Methods of Soil Analysis, Part 4—Physical Methods. Soil Science Society of America, Inc., Madison, WI, USA, pp. 229–240.

Gee, G.W., Bauder, J.W., 1986. Particle-size analysis. In: Klute, A. (Ed.), Methods of Soil Analysis Part I, Physical and Mineralogical Methods. Soil Science Society of America, Madison, WI, USA, pp. 383–412.

Goldshleger, N., Ben-Dor, E., Benyamini, Y., Agassi, M., 2004. Soil reflectance as a tool for assessing physical crust arrangement of four typical soils in Israel. Soil Sci. 169 (10), 677–687.

Hair Jr., J.F., Anderson, R.E., Tatham, R.L., Black, W.C., 1995. Multivariate data analysis. Prentice Hall, Englewood Cliffs, New Jersey.

Henderson, T.L., Szilagyi, A., Baumgardner, M.F., Chen, C.T., Landgrebe, D.A., 1989. Spectral band selection for classification of soil organic matter content. Soil Sci. Soc. Am. J. 53, 1778–1784.

Hills, R.G., Hudson, D.B., Wierenga, P.J., 1992. Spatial variability at the Las Cruces Trench site. In: van Genuchten, M.Th., Leij, F.J. (Eds.), Proceedings of the International Workshop on Indirect Methods for Estimating the Hydraulic Properties of Unsaturated Soils, Riverside, California, USA, pp. 529–538.

Hodnett, M.G., Tomasella, J., 2002. Marked differences between van Genuchten soil water-retention parameters for temperate and tropical soils: a new water-retention pedotransfer functions developed for tropical soils. Geoderma 108, 155–180.

ICAR, 2006. Soil. Handbook of Agriculture. Indian Council of Agricultural Research, New Delhi, India.

Islam, K., Singh, B., McBratney, A., 2003. Simultaneous estimation of several soil properties by ultra-violet, visible, and near infrared reflectance spectroscopy. Aust. J. Soil Res. 41 (6), 1101–1114.

Jana, R.B., Mohanty, B.P., Springer, E.P., 2007. Multiscale pedotransfer functions for soil water retention. Vadose Zone J. 06, 868–878.

Jana, R.B., Mohanty, B.P., Springer, E.P., 2008. Multiscale Bayesian neural networks for soil water content estimation. Water Resour. Res. 44, W08408. doi:10.1029/2008WR006879.

Janik, L.J., Merry, R.H., Forrester, S.T., Lanyon, D.M., Rawson, A., 2007. Rapid prediction of soil water retention using mid infrared spectroscopy. Soil Sci. Soc. Am. J. 71, 507–514.

Klute, A., Dirksen, C., 1986. Hydraulic conductivity and diffusivity: laboratory methods, In: Klute, A. (Ed.), Methods of Soil Analysis. Part 1, 2nd ed.: Agron. Monogr., vol. 9. ASA and SSSA, Madison, WI, pp. 687–734.

Lagacherie, P., Baret, F., Feret, J.B., Madeira Netto, J., Robbez-Masson, J.M., 2008. Estimation of soil clay and calcium carbonate using laboratory, field, and airborne hyperspectral measurements. Remote Sens. Environ. 112 (3), 825–835.

Lee, D.M., Reynolds, W.E., Elrich, D.E., Clothiers, B.E., 1985. A comparison of three field methods for measuring saturated hydraulic conductivity. Can. J. Soil Sci. 65, 563–573.

Leone, A.P., Sommer, S., 2000. Multivariate analysis of laboratory spectra for the assessment of soil development and soil degradation in the Southern Apennines (Italy). Remote Sens. Environ. 72, 346–359.

Li, Y., Chen, D., White, R.E., Zhu, A., Zhang, J., 2007. Estimating soil hydraulic properties of Fengiu county soils in the North China Plain using pedotransfer functions. Geoderma 138 (3–4), 261–271.

McBratney, A.B., Minasny, B., Cattle, S.R., Vervoort, R.W., 2002. From pedotransfer functions to soil inference systems. Geoderma 109, 41–73.

McCarty, G.W., Reeves III, G.B., Reeves, V.B., Follett, R.F., Kimble, J.M., 2002. Mid-infrared and near-infrared diffuse reflectance spectroscopy for soil carbon measurement. Soil Sci. Soc. Am. J. 66, 640–646.

Minasny, B., McBratney, A.B., 2002. The neuro-m method for fitting neural network parametric pedotransfer functions. Soil Sci. Soc. Am. J. 66, 352–361.

Minasny, B., Hopmans, J.W., Harter, T., Eching, S.O., Tuli, A., Denton, M.A., 2004. Neural network predictions of soil hydraulic functions for alluvial soils using multistep outflow data. Soil Sci. Soc. Am. J. 68, 417–429.

Mouazen, A.M., Maleki, M.R., Baerdemaeker, J.D., Ramon, H., 2007. On-line measurement of some selected soil properties using a VIS-NIR sensor. Soil Tillage Res. 93, 13–27.

Nanni, M.R., Demattê, J.A.M., 2006. Spectral reflectance methodology in comparison to traditional soil analysis. Soil Sci. Soc. Am. J. 70, 393–407.

NBSS&LUP, 2005. Soil Series of Orissa. National Bureau of Soil Survey and Land Use Planning, Nagpur, India.

Nemes, A., Rawls, W.J., Pachepsky, Ya.A., 2006. Use of the non-parametric nearest neighbor approach to estimate soil hydraulic properties. Soil Sci. Soc. Am. J. 70, 327–336.

Odlare, M., Svensson, K., Pell, M., 2005. Near infrared reflectance spectroscopy for assessment of spatial soil variation in an agricultural field. Geoderma 126, 193–202.

Pachepsky, Ya.A., Timlin, D.J., Rawls, W.J., 2001. Soil water retention as related to topographical variables. Soil Sci. Soc. Am. J. 65, 1787–1795.

Pachepsky, Y.A., Rawls, W.J., Lin, H.S., 2006. Hydropedology and pedotransfer functions. Geoderma 131, 308–316.

Paige, G.B., Hillel, D., 1993. Comparison of three methods for assessing soil hydraulic properties. Soil Sci. 155, 175–189.

Rawls, W.J., Brakensiek, D.L., Saxton, K.E., 1982. Estimation of soil water properties. Trans. ASAE 25, 1316–1320.

Rawls, W.J., Gish, T.J., Brakensiek, D.L., 1991. Estimating soil water retention from soil physical properties and characteristics. Adv. Soil Sci. 16, 213–234.

Reeves, J., McCarty, G., Mimmo, T., 2002. The potential of diffuse reflectance spectroscopy for the determination of carbon inventories in soils. Environ. Pollut. 116, 277–284.

Romano, N., Palladino, M., 2002. Prediction of soil water retention using soil physical data and terrain attributes. J. Hydrol. 265, 56–75.

Santra, P. 2009. Delineation and characterization of hydrologically-similar zones based on spatial distribution of soil hydraulic properties. PhD thesis. Indian Institute of Technology, Kharagpur.

Santra, P., Das, B.S., 2008. Pedotransfer functions for soil hydraulic properties developed from a hilly watershed of Eastern India. Geoderma 146, 439–448.

Schaap, M.G., Leij, F.J., van Genuchten, M.Th., 1998. Neural network analysis for hierarchical prediction of soil hydraulic properties. Soil Sci. Soc. Am. J. 62, 847–855.

Schaap, M.G., Leij, F.J., van Genuchten, M.Th., 2001. Rosetta: a computer program for estimating soil hydraulic parameters with hierarchical pedotransfer functions. J. Hydrol. 251, 163–176.
Scheinost, A.C., Sinowski, W., Auerswald, A., 1997. Regionalization of soil water retention curves in a highly variable soilscape, I. Developing a new pedotransfer function. Geoderma 78, 129–143.
Sharma, S.K., Mohanty, B.P., Zhu, J., 2006. Including topograph and vegetation attributes for developing pedotransfer functions. Soil Sci. Soc. Am. J. 70, 1430–1440.
Shepherd, K.D., Walsh, M.G., 2002. Development of reflectance spectral libraries for characterization of soil properties. Soil Sci. Soc. Am. J. 66, 988–998.
Šimunek, J., Angulo-Jaramillo, R., Schaap, M.G., Vandervaere, J., van Genuchten, M.T., 1998. Using an inverse method to estimate the hydraulic properties of crusted soils from tension-disc infiltrometer data. Geoderma 86, 61–81.
Stevens, A., van Wesemael, B., Vandenshrick, G., Toure, S., Tychon, B., 2006. Detection of carbon stock changes in agricultural soil using spectroscopic techniques. Soil Sci. Soc. Am. J. 70, 844–850.
Tamari, S., Wösten, J.H.M., 1999. Using artificial neural networks to develop pedotransfer functions of soil hydraulic conductivity. In: van Genuchten, M.Th., et, al. (Eds.), Proceedings of the International Workshop on Characterization and Measurement of the Hydraulic Properties of Unsaturated Porous Media. University of California, Riverside, CA, pp. 1251–1260.
Thine, C., Shephered, K., Walsh, M., Coe, R., Okwach, G., 2004. Application of GIS and Remote Sensing in Characterization of Soil Hydraulic Properties for Soil Physical Quality Assessment. Univeristy of Nairobi, Kenya, pp. 1–18.
Tomasella, J., Hodnett, M.G., 1998. Estimating soil water retention characteristics from limited data in Brazilian Amazonia. Soil Sci. 163, 190–202.
Van Genuchten, M.Th., 1980. A close-form equation for predicting the hydraulic conductivity of unsaturated soils. Soil Sci. Soc. Am. J. 44, 892–898.
Vereecken, H., Maes, J., Feyen, J., Darius, P., 1989. Estimating the soil moisture retention characteristics from texture, bulk density and carbon content. Soil Sci. 148, 389–403.
Viscara Rosel, R.A., Walvoort, D.J.J., McBratney, A.B., Janik, L.J., Skjemstad, J.O., 2006. Visible, near infrared, mid infrared or combined diffuse reflectance spectroscopy for simultaneous assessment of various soil properties. Geoderma 131, 59–75.
Walkley, A.J., Black, I.A., 1934. An examination of Degtjareff method for determining soil organic matter and a proposed modification of the chromic acid titration method. Soil Sci. 37, 29–38.
Wösten, J.H.M., Lilly, A., Nemes, A., Le Bas, C., 1999. Development and use of a database of hydraulic properties of European soils. Geoderma 90, 169–185.
Wösten, J.H.M., Pachepsky, Ya.A., Rawls, W.J., 2001. Pedotransfer functions: bridging the gap between available basic soil data and missing soil hydraulic characteristics. J. Hydrol. 251, 123–150.